

## Availability of High-Quality TRMM Ground Validation Data from Kwajalein, RMI: A Practical Application of the Relative Calibration Adjustment Technique

DAVID A. MARKS, DAVID B. WOLFF, AND DAVID S. SILBERSTEIN

*Laboratory for Atmospheres, NASA Goddard Space Flight Center, Greenbelt, and Science Systems and Applications, Inc., Lanham, Maryland*

ALI TOKAY

*Laboratory for Atmospheres, NASA Goddard Space Flight Center, Greenbelt, and Joint Center for Earth Systems Technology, University of Maryland, Baltimore County, Baltimore, Maryland*

JASON L. PIPPITT AND JIANXIN WANG

*Laboratory for Atmospheres, NASA Goddard Space Flight Center, Greenbelt, and Science Systems and Applications, Inc., Lanham, Maryland*

(Manuscript received 19 May 2008, in final form 11 August 2008)

### ABSTRACT

Since the Tropical Rainfall Measuring Mission (TRMM) satellite launch in November 1997, the TRMM Satellite Validation Office (TSVO) at NASA Goddard Space Flight Center (GSFC) has been performing quality control and estimating rainfall from the KPOL S-band radar at Kwajalein, Republic of the Marshall Islands. Over this period, KPOL has incurred many episodes of calibration and antenna pointing angle uncertainty. To address these issues, the TSVO has applied the relative calibration adjustment (RCA) technique to eight years of KPOL radar data to produce Ground Validation (GV) version 7 products. This application has significantly improved stability in KPOL reflectivity distributions needed for probability matching method (PMM) rain-rate estimation and for comparisons to the TRMM precipitation radar (PR). In years with significant calibration and angle corrections, the statistical improvement in PMM distributions is dramatic. The intent of this paper is to show improved stability in corrected KPOL reflectivity distributions by using the PR as a stable reference. Intermonth fluctuations in mean reflectivity differences between the PR and corrected KPOL are on the order of  $\pm 1$ – $2$  dB, and interyear mean reflectivity differences fluctuate by approximately  $\pm 1$  dB. This represents a marked improvement in stability with confidence comparable to the established calibration and uncertainty boundaries of the PR. The practical application of the RCA method has salvaged eight years of radar data that would have otherwise been unusable and has made possible a high-quality database of tropical ocean-based reflectivity measurements and precipitation estimates for the research community.

### 1. Introduction

There are many applications in which quantitative rainfall estimation is essential. From station climatology to validation of satellite algorithms, the estimation of rainfall using ground-based radar is a necessity. A stable and well-calibrated radar is an absolute requirement for robust rainfall estimation (Ulbrich and Lee 1999). This

is certainly true in tropical oceanic regions where rain gauge measurements are sparse and where polar-orbiting satellite overpass revisit times are less frequent than at higher latitudes. The Kwajalein oceanic region in the Republic of the Marshall Islands (Fig. 1) is one of several unique Ground Validation (GV) locations for Tropical Rainfall Measuring Mission (TRMM) validation studies (Schumacher and Houze 2000; Houze et al. 2004; Wolff et al. 2005; Yuter et al. 2005), mesoscale and physical characterization studies (Sobel et al. 2004; Cetrone and Houze 2006; Holder et al. 2008), cloud-resolving model simulations (Blossey et al. 2007), and

---

*Corresponding author address:* David A. Marks, NASA GSFC, Code 613.1, Greenbelt, MD 20771.  
E-mail: david.a.marks@nasa.gov

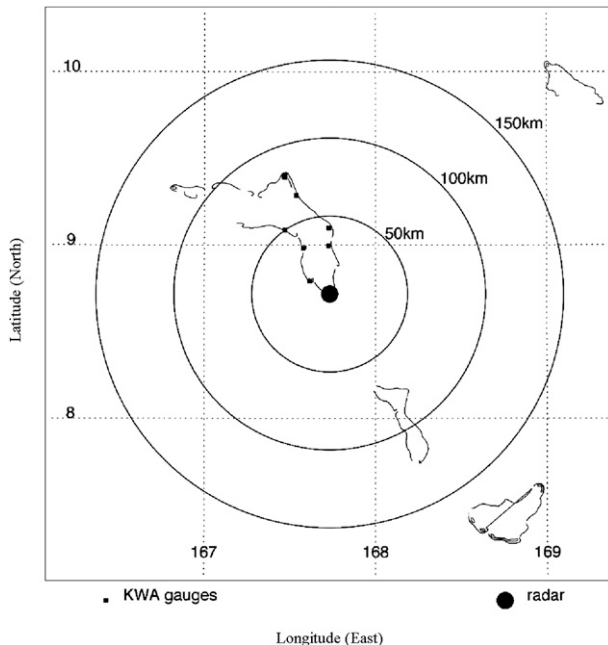


FIG. 1. The location of Kwajalein Island in the Republic of the Marshall Islands (from Wolff et al. 2005). The KPOL S-band radar is located at the center of the image. Rain gauge locations from the KWA network are shown as black squares.

other research topics. The National Aeronautics and Space Administration (NASA)-supported KPOL S-band weather radar located on Kwajalein Island (8.7°N, 167.7°E) is a vital tool in these efforts. KPOL task configurations are shown in Table 1, and additional radar characteristics are found in Schumacher and Houze (2000, their Table 1), and Wolff et al. (2005, their Table 1). The virtually complete oceanic coverage in this remote location makes data from the Kwajalein GV site highly desirable; however, technical and logistical concerns have often pushed data quality issues to the forefront. Concerns regarding KPOL calibration and overall stability have repeatedly compromised attempts to provide accurate and consistent reflectivity measurements and rain-rate estimates. KPOL radar sensitivity has fluctuated for a variety of reasons including mechanical and engineering issues (e.g., failed parts in harsh environmental conditions), software instability, abrupt power adjustments, and antenna pointing angle changes. It became obvious that a method was needed to first detect these changes and then quantify the impact on the data itself before useful validation products could be provided. The relative calibration adjustment (RCA) and monitoring technique (Silberstein et al. 2008, hereafter SW08) detects and quantifies radar sensitivity changes to within an accuracy of  $\pm 0.5$  dB. In the practical application of RCA theory, ensemble KPOL

TABLE 1. Task configuration of the KPOL radar. Columns are task name, radar polarization, elevation angles (deg), and pulse repetition frequency (PRF). The volume scans alternate between A and B, with one surveillance scan between volume scan sets. Volume and surveillance scan completion times are 5:25 (min:s) and 0:53, respectively. There are 10 volume scans per hour (5 A scans and 5 B scans) and 240 total volume scans per day (if 100% operational).

Task	Polarization	Elevation angles (deg)	PRF
GVVOL_A	Dual	0.4, 1.4, 2.3, 4.2, 6.1, 8.0, 9.9, 11.8, 14.0, 16.6, 19.6, 23.2	960
GVVOL_B	Dual	0.4, 1.4, 3.3, 5.2, 7.1, 9.0, 10.9, 12.9, 15.2, 18.0, 21.3, 25.3	960
Surv_TRMM	Horizontal	0.4	396

data from locations with persistent ground clutter signatures are objectively analyzed to routinely detect, monitor, and quantify radar sensitivity fluctuations, antenna elevation changes, and overall KPOL status in a near-real-time operational environment. The scope of this paper is to (i) describe frequently encountered KPOL radar and data issues, (ii) explain historical data correction attempts and limitations, (iii) examine the practical application of RCA theory, (iv) provide a comparison between RCA and other correction methods, and (v) quantitatively show the significantly improved stability of the corrected radar data and resulting statistical consistency from the window probability matching method (WPMM; Rosenfeld et al. 1994) in reflectivity–rain-rate relation development.

## 2. Frequently encountered issues and historical TRMM Satellite Validation Office correction attempts

### a. Early TRMM Satellite Validation Office processing

The KPOL radar has a long history of problems that have run the gamut from hardware and software failure to unplanned or undocumented antenna elevation angle changes. From 2000 through 2007, KPOL's performance has been dominated by time periods of relative stability punctuated by sharp sensitivity (power calibration) and elevation angle changes. KPOL radar sensitivity has changed frequently and for various reasons as shown in Houze et al. (2004, their Table 2). Mechanical and engineering issues such as waveguide pressurization leaks with subsequent arcing, replacement of directional couplers with suspected incomplete follow-through procedures, pulse-forming network replacements, elevation and azimuth drive motor failures, unexplained antenna gain changes, and general calibration

drift have all occurred within the extremely harsh environmental conditions that define this region. Elevation angle changes have been caused by a suspected faulty electrical panel with spliced connections and the use of a problematic release of a solar tracking utility.

Historical attempts to quantify the effect of sensitivity/calibration changes have shown only modest success. Because limited engineering documentation was available from KPOL, early versions of the TRMM Satellite Validation Office (TSVO) products (through version 4) concentrated more on adjusting reflectivity to match rain gauge rainfall rates rather than correcting the reflectivity field itself. These versions used the “bulk-adjustment” technique to force agreement between radar reflectivity and rain gauge measurements (Marks et al. 2000; Amitai et al. 2006). As explained in Amitai et al. (2006), guidelines from the prelaunch TRMM GV Science Team specified the use of rain gauge-adjusted power-law relations of the form

$$Z_e = AR^b, \quad (1)$$

with fixed exponent  $b = 1.4$ . In this context,  $Z_e$  is the effective (or observed) reflectivity.<sup>1</sup> A network of quality-controlled gauges was used to tune the power-law coefficient  $A$  such that total *monthly* rainfall, as estimated from the radar  $Z_e$  pixels above the gauges, was matched to the combined gauge accumulations ( $\Sigma G$ ):

$$A = \left[ \frac{\sum (Z_e^{1/b})}{\sum G} \right]^b. \quad (2)$$

Rain gauge data were interpolated and quality controlled via a cubic spline-based method described in Wang et al. (2008). Separate monthly convective and stratiform  $Z_e$ - $R$  relations were generated using the reflectivity classification criteria defined in Steiner et al. (1995). Within the KPOL field of view, there are only 15 rain gauge sites. Seven locations are shown in Wolff et al. (2005), and the additional eight comprise the X-array at Roi-Namur Island (approximately 80 km north of the KPOL site). Data from six of the X-array gauges became available in April 2003, and the additional two in April 2005. By the bulk-adjustment method, known and unknown radar calibration adjustments were incorporated into radar estimated rain rates, but the TRMM standard products (TSP) 1C-51 and 2A-55 (see Table 4 in Wolff et al. 2005 for product descriptions) did

not contain calibration-corrected reflectivity. The resulting wide variations in  $Z_e$ - $R$  relationships (in-house study) clearly showed that egregious inconsistencies existed between observed reflectivity and gauge rain rates.

#### b. TSVO version 5 processing

In the progression to TSVO version 5 (V5) validation products, the monthly bulk-adjustment and power-law method was abandoned in favor of WPMM to statistically match radar and rain gauge data for derivation of  $Z_e$ - $R$  lookup tables. To obtain sufficient sample sizes for WPMM, monthly observations of radar and rain gauge pairs were combined for an entire year without regard to classification. The official (operational) V5 products for Kwajalein used a fixed WPMM derived  $Z_e$ - $R$  lookup table (derived from year 2002 reflectivity and rain gauge data) for rain-rate estimation but still had no reflectivity calibration adjustments (Wolff et al. 2005). Reflectivity distributions for WPMM were from a SPRINT-interpolated (Mohr and Vaughan 1979) constant altitude plan-position indicator (CAPPI) level of 1.5 km, and the rain gauge data were interpolated and quality controlled via the cubic spline-based method described in Wang et al. (2008). Based on available KPOL engineering information that implied reflectivity from year 2002 was very stable, the entire year of data was chosen for development of an operational WPMM  $Z_e$ - $R$  table. However, essential to this study's comparison to later product versions (6 and 7), separate yearly WPMM  $Z_e$ - $R$  lookup tables were generated from years 2000 through 2007. Although the WPMM does not require certainty in the *absolute* calibration of the radar, it definitely requires stability in the *relative* calibration. Statistical inconsistencies develop if the relative radar calibration is absent. Figure 2 shows the divergence in yearly  $Z_e$ - $R$  lookup tables from the V5 methodology, and Table 2 shows the associated *approximate* power-law  $A$  coefficients derived for each year. [The version 6 (V6) and 7 (V7) coefficients in Table 2 are discussed in section 3b.] The diverging curves and coefficients indicate distinctly different interannual WPMM reflectivity distributions. We believe these differences lack a physical rationale.

Disdrometer studies indicate that reflectivity distributions in the Kwajalein climatic regime show very little variation in both temporal and spatial scales (Schumacher and Houze 2000). The north-south oscillation of the intertropical convergence zone (ITCZ) primarily dominates the precipitation for the entire region. Employing 2 yr of disdrometer observations in Kwajalein, the composite raindrop spectra were constructed at the 40-dBZ interval ( $\pm 0.5$  dB) for four different rain events (Fig. 3a). The disdrometer was an impact type (Joss and

<sup>1</sup> The radar-measured or effective reflectivity  $Z_e$  is an average of the distribution of the actual reflectivity  $Z$  of the targets within the volume illuminated by the radar beam, weighted by the beam radiation pattern (Probert-Jones 1962; Rosenfeld et al. 1992).

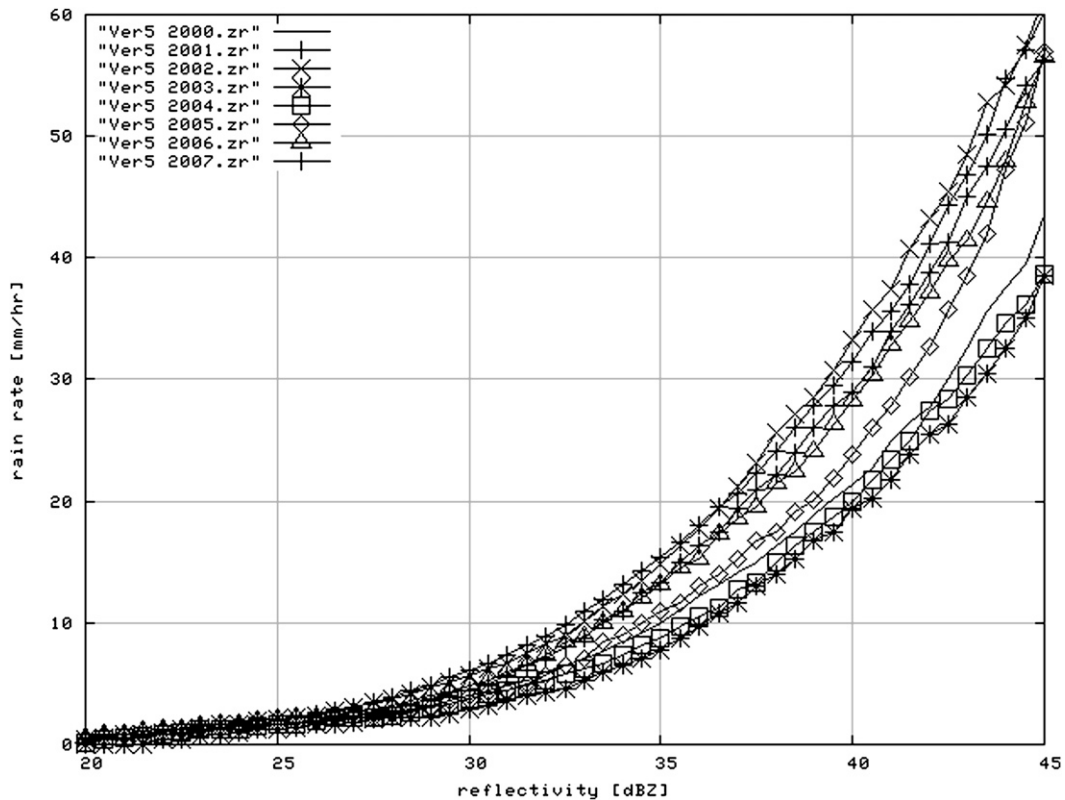


FIG. 2. TSVO GV V5 WPMM yearly  $Z_e$ - $R$  curves, 2000-07. Divergence in  $Z_e$ - $R$  curves signifies that relative stability in reflectivity distributions from year to year does not exist.

Waldvogel 1967) and the reflectivity was calculated from 1-min disdrometer observations. We intentionally selected the 40-dBZ interval, below which the size spectra are narrow in the absence of large drops and where intrastorm variability (e.g., convective versus stratiform

TABLE 2. Approximated  $Z_e$ - $R$  power-law  $A$  coefficients by year and TSVO GV product version number. V5 coefficients have no calibration or elevation corrections applied. V6 coefficients have calibration adjustments applied but no account is made for changes in antenna elevation. V7 coefficients incorporate both RCA and correctly applied elevation adjustments. The yearly coefficients show much better agreement in V7, providing further evidence that statistical consistency has been improved. In all versions and years, the exponent of the power-law approximation is 1.4.

Year/version	V5	V6	V7
2000	158	129	129
2001	92	132	132
2002	95	101	155
2003	204	76	147
2004	172	108	132
2005	136	50	135
2006	111	512	168
2007	110	231	180

rainfall) may occur, and above which the sample size is very limited (less than five 1-min observations). The agreement in composite spectra between the different events is evident. The presence of high concentrations of small drops and low concentrations of large drops resulted in a higher total number of concentrations, liquid water content, and rain rate than extratropical cyclones (Tokay et al. 2008). All three integral parameters that were shown in Fig. 3a were calculated from observed spectra. We repeated the same exercise employing 1 yr of Roi-Namur disdrometer observations. Figure 3b shows the composite spectra at 40 dBZ from three different events. Again, the agreement in composite spectra between the events as well as between the Kwajalein and Roi-Namur locations is evident. This suggests that for a given reflectivity, one should expect a very narrow range of rain rate and therefore a single  $Z_e$ - $R$  relation may be relevant in the absence of interstorm variability.

The year-to-year reflectivity distribution differences of V5 shown in Fig. 2 and Table 2 indicate probable instability in relative radar calibration. To quantify the yearly variation in V5 reflectivity distributions, we compared the mean reflectivity with a recognized stable

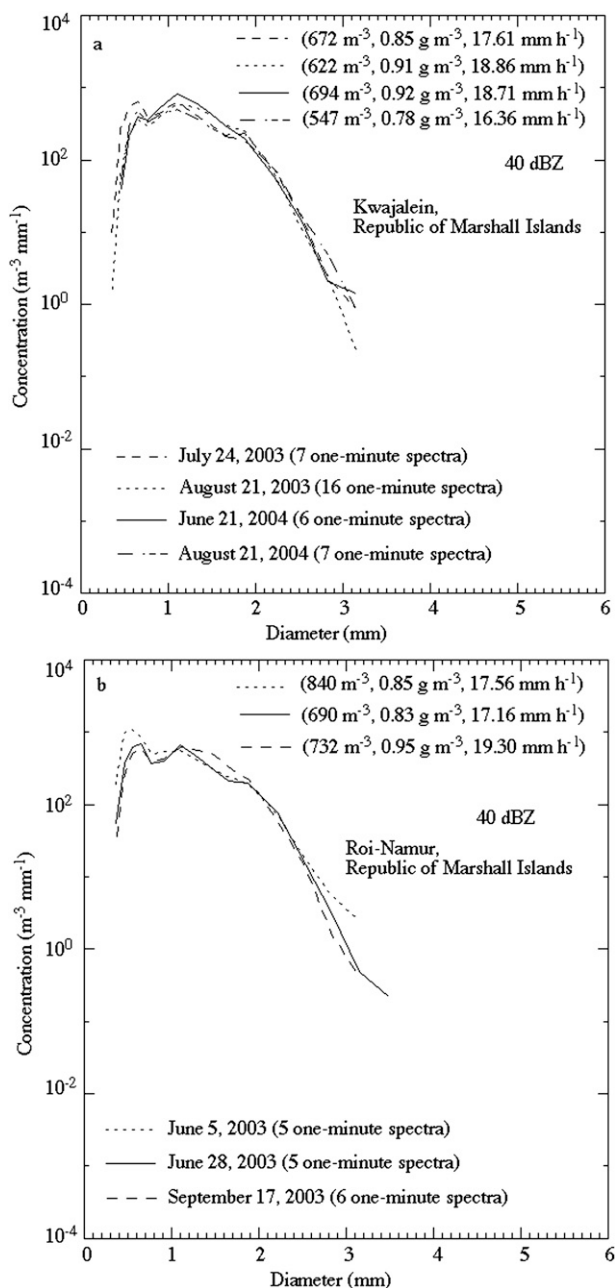


FIG. 3. Composite raindrop spectra at 40 dBZ (a) from four rain events in two different years in Kwajalein and (b) from three events in Roi-Namur. The number of 1-min disdrometer observations in each rain event is given. The disdrometer-calculated total number of drops, liquid water content, and rain rate are also given for each rain event.

standard, the TRMM precipitation radar (PR). It has been demonstrated that the TRMM PR is consistent in calibration stability [with a large signal-to-noise (S/N) ratio] to within 0.8 dB (Kozu et al. 2001), with an estimated uncertainty in the reflectivity factor of less than

1.0 dB (Kummerow et al. 1998; Iguchi et al. 2000). This level of stability provides a reference to quantify the resultant instability of the TSVO KPOL V5 reflectivity. TSP 2A-55 (Wolff et al. 2005, their Table 4) is a three-dimensional Cartesian gridded (via SPRINT; Mohr and Vaughan 1979) quality-controlled reflectivity product with a resolution of  $151 \times 151 \times 13$  pixels [ $2 \text{ km} \times 2 \text{ km}$  horizontal, 1.5 km vertical, with 13 constant altitude plan-position indicator (CAPPI) height levels]. Mean attenuation-corrected reflectivities from PR 2A25 V6 were compared with mean ground radar reflectivities from KPOL 2A55 V5. For this comparison, both KPOL and PR reflectivity data were resampled to a three-dimensional Cartesian grid with  $4 \text{ km} \times 4 \text{ km}$  horizontal and 1.5 km vertical resolution. The Cartesian origin was centered at the KPOL site with a horizontal extent of 150 km and vertical range from 0 to 20 km. Only data classified as stratiform were included, where classification was obtained by the 2A23 algorithm for the PR (Awaka et al. 1997) and the 2A54 algorithm for KPOL (Steiner et al. 1995). These comparisons used data  $\geq 18$  dBZ to be above the PR sensitivity threshold, from multiple heights to minimize uncertainties associated with sampling resolutions, and within 8-min time windows of the PR scan time [ $-1 \text{ min} \leq (\text{PR}_{\text{time}} - \text{KPOL}_{\text{time}}) \leq +7 \text{ min}$ ]. This was a direct comparison of mean reflectivity measurements at multiple levels from both instruments; it is similar to the method of Anagnostou et al. (2001, hereafter AMD01). There are numerous sources of error when comparing reflectivity from space-based with ground-based radar (Bolen and Chandrasekar 2000; Bolen and Chandrasekar 2003), including consideration of different view angles, beam-widths, frequencies, noise floors, hydrometeor distributions, time synchronization mismatches, and interpolation errors, among others. Bolen and Chandrasekar (2000) performed a theoretical comparison of reflectivity at S and Ku bands (assuming no relative calibration bias between the radars) and showed that theoretical reflectivity differences (S band - K band) could range from  $\pm 0.5$  dB within bounds of one standard deviation. To complement that study, Bolen and Chandrasekar (2003) developed a method to align and compare spaceborne and ground-based radar observations with an emphasis on volume matching and geometric corrections. Application of their method to data from the Texas-Florida Underflights (TEFLUN-B) field campaign (August 1998) with the NCAR SPOL radar and to KPOL data from July 2000 showed that their method minimizes spaceborne and ground-based comparison errors; however, proper calibration of the ground-based radar is of crucial importance. Measurement uncertainty in the PR reflectivity is approximately 1 dB, whereas uncertainty in the uncalibrated

and unstable V5 KPOL reflectivity measurements is a significant variable. Indeed, KPOL calibration was low by approximately 6 dB (as compared to the PR) at the start of the Kwajalein Experiment (KWAJEX) field campaign (Yuter et al. 2005) and has fluctuated significantly since then (discussed in the following section); accordingly, we expected high standard deviations about the mean differences between the instruments. V5 comparison results showed interyear (2000–07) standard deviations about the mean differences in reflectivity ranging from 3.5 to 4.3 dB. If the KPOL radar calibration had been stable, we would in theory expect measurement error of approximately  $\pm 1$  dB. Combined with the uncertainty of the PR, the expected error associated with this type of comparison is approximately  $\pm 2$  dB. The *fluctuation* of the mean differences between instruments is much more important to this study than the absolute magnitude of the differences themselves because it is this fluctuation that quantifies the degree of instability in V5 reflectivity. The multiple panels of Fig. 4 show monthly and yearly mean reflectivity differences (offsets) between TRMM PR 2A25 V6 and KPOL 2A55 V5 for rainy overpasses from 2000 through 2007 and indicate years of both relative stability and extreme instability. Monthly fluctuations in mean reflectivity differences over the eight years are quite evident and are on the order of several decibels, especially in 2000, 2001, and 2003. In contrast, mean differences show very little fluctuation from May through December 2004. Months with no information represent periods in which the KPOL radar was extremely unstable and have therefore been removed. Data from August through December 2005 were removed because of multiple cascading KPOL component failures. The wide variation in reflectivity distributions is also reflected in the yearly mean differences shown in the final column in each yearly panel and is on the order of  $\pm 2$  dB. On the yearly scale there are thousands of  $4 \text{ km} \times 4 \text{ km}$  pixels being compared; they range from about 13 000 in 2005 to more than 60 000 in 2002. The 95% confidence interval (95% CI) of the yearly mean differences (to two significant figures) is nearly 0.0. The 95% CI is derived from construction of a Student's  $t$  test statistic (Wilks 1995):

$$95\% \text{ CI} = \left( \bar{O} - t_{\alpha/2} \frac{s}{\sqrt{n}}, \bar{O} + t_{\alpha/2} \frac{s}{\sqrt{n}} \right), \quad (3)$$

where  $\bar{O} = (1/n) \sum_n (R_{\text{PR}} - R_{\text{KPOL}})$ ,  $\alpha$  is the statistical significance level of 5%,  $t_{\alpha/2}$  is the  $100(\alpha/2)$ th percentile of the  $t$  distribution with  $n - 1$  degrees of freedom,  $s$  is the sample standard deviation of the individual offset ( $O$ ) values, and  $n$  is the sample size when both  $R_{\text{PR}}$  and  $R_{\text{KPOL}} \geq 18 \text{ dBZ}$ . The sample sizes on the monthly scale

can be significantly smaller in the dry season of each year (January–March) when precipitation is mainly dominated by isolated to scattered showers. This is shown in Fig. 4 by extreme fluctuations in mean differences, and lower confidence levels (larger 95% CI bounds) in these three months. The level of instability shown in the V5 reflectivity statistics and the  $Z_e$ – $R$  curve divergence are unacceptable for consistent rain-rate estimation. A technique to identify, quantify, and monitor relative calibration changes to radar reflectivity over persistent ground clutter areas was developed by the TSVO to provide the required stability.

### 3. Relative calibration adjustment theory and practical application

#### a. RCA theory

Unlike studies using a single source of continuous ground clutter (Rinehart 1978), the RCA technique uses a statistical ensemble of reflectivity values ( $Z_e$  in dBZ) from persistent ground clutter areas from every volume scan to monitor hourly and daily radar sensitivity changes. As detailed in SW08, the 95th percentile of the clutter area reflectivity distribution at the lowest elevation scan has been found to be remarkably stable from hour to hour, day to day, and month to month to within  $\pm 0.5$  dB. It varies significantly only after deliberate system modifications, equipment failure, or other causes, some of which may be unknown. Selecting the 95th percentile of the cumulative distribution function (CDF) associated with intense clutter reflectivities permits monitoring of radar stability (SW08). This is because almost all precipitation echoes are below the 95th percentile level. Any transient rain echoes that approach the 95th percentile reflectivity level are statistically insignificant on an hourly or daily basis relative to the ground clutter. The definition of a relative calibration adjustment is the amount (in dB) needed to force agreement between the 95th percentile reflectivity distribution and the established calibration baseline. The reflectivity level at which the CDF attained 95% defined our initial reference (baseline) and was determined in part by a consensus of engineers and researchers from the University of Washington (UW), NASA, and Colorado State University (CSU) with data from the KWAJEX field campaign (Yuter et al. 2005). The original uncalibrated 95th percentile reflectivity distribution value on 1 August 1999 was 44 dBZ. As explained in section 4, a calibration adjustment of +6 dB was required. This brought the initial calibrated baseline to 50 dBZ. As described in SW08, the ability of the RCA method to detect changes in radar sensitivity

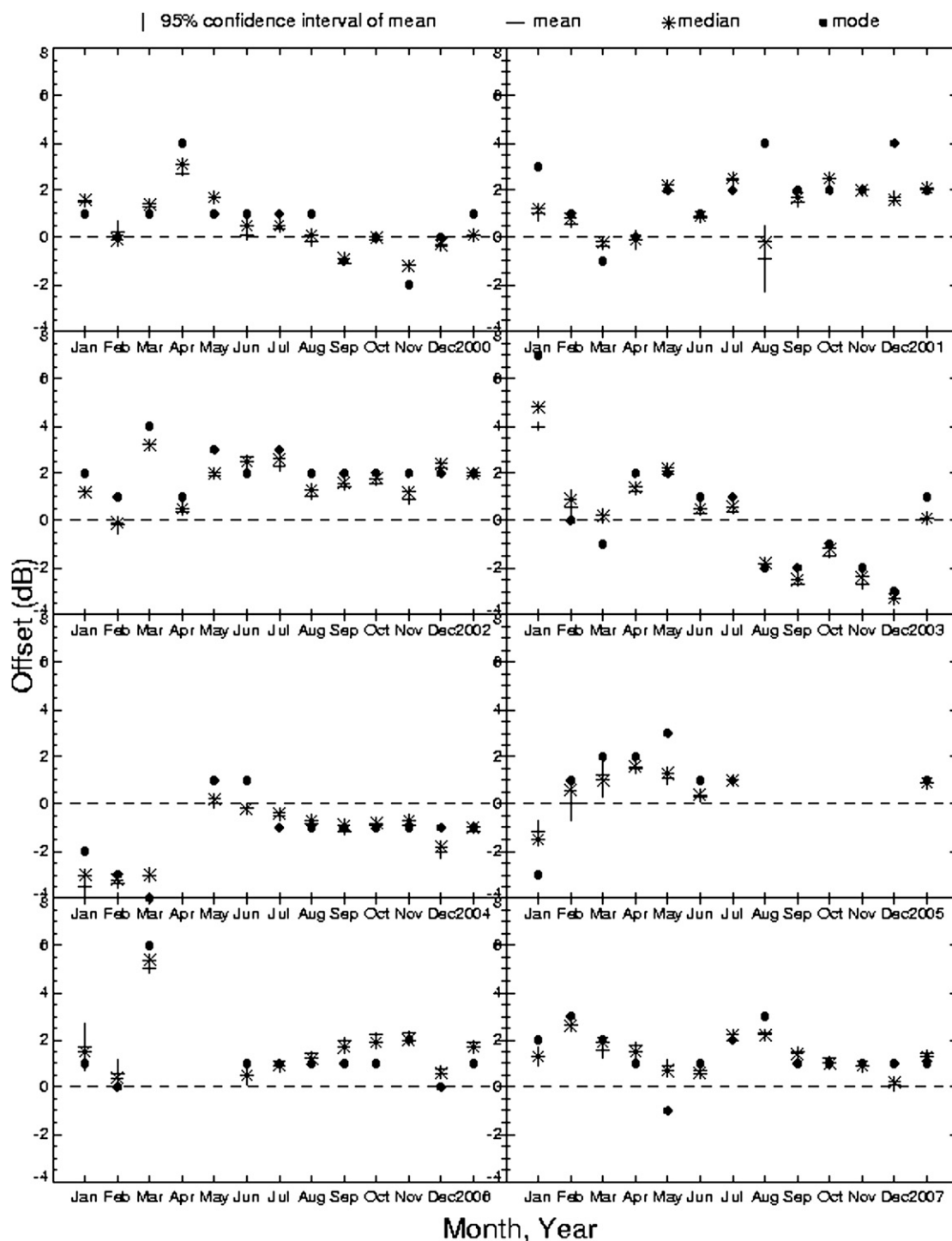


FIG. 4. Monthly and yearly comparison of mean reflectivity difference (offset) between the TRMM PR (2A25; V6) and TSVO KPOL (2A55; V5) for years 2000–07. The final column in each panel is for the entire year. Increased offsets in January through March of each year are related to limited sample size in the dry season.

was validated (with KPOL operator assistance) and showed a direct one-to-one correspondence between KPOL calibration offset changes and ensemble 95th percentile reflectivity distributions.

Probability and cumulative distribution functions (PDFs and CDFs) of reflectivity over the ensemble clutter locations are obtained on an hourly and daily basis to determine an RCA value and include both the

precipitation and clutter echoes. Figure 5 is a three-panel plot showing the hourly and daily PDF and CDF plots of clutter area reflectivity from a stable calibration day, a problem calibration day, and an antenna elevation irregularity day. Figure 5a (stable calibration day) has hour-to-hour RCA fluctuations less than 0.5 dB, and the calibration stability is graphically shown by the convergence in reflectivity distributions at the 95th percentile (approximately 50 dBZ). The distribution spread below this level is the result of light precipitation echo and variations in the clutter field. Figure 5b (problem calibration day) has a significant jump ( $> 5$  dB) in the hourly RCA values between 0100 and 0300 UTC. Not enough data points were available for a valid distribution during the 0200 UTC hour (therefore the  $-99.99$  flag). Divergence in the 95th percentile hourly reflectivity distributions is clearly evident in both the PDF and CDF analysis and signifies that a sensitivity change has occurred. Review of engineering logs and correspondence with radar operators confirmed that a directional coupler had been swapped during the 0200 UTC hour and that calibration follow-through procedures were not completed, thereby affecting the calibration. Figure 5c (antenna elevation irregularity day) shows a significant fluctuation ( $> 4$  dB) in the RCA value from the 2200 to 2300 UTC hour. There were no known engineering issues affecting power on this day, so it was suspected that the antenna elevation angle had changed for an unknown reason. A different type of analysis was needed to diagnose the possible antenna elevation problem.

When attempting to diagnose radar elevation angle irregularities, a very useful method is to rank individual gate returns in order of descending reflectivity. In a nominal, stable configuration, the most intense reflectivity values will be situated across a range of distances encompassing points both near and far from the radar. However, if the radar elevation angle deviates from its typical orientation, the distances at which the most intense reflectivities are found vary significantly. In the case of a higher than normal elevation angle, the most intense points tend to cluster within a few kilometers of the radar because targets at farther range are missed because of beam overshoot. In the case of a lower than normal elevation angle, the location of the most intense reflectivities tends to be at greater distances from the radar than the nominal case as more distant targets are captured within the radar beam. Although this method tends to work best for more severe angular deviations (on the order of several tenths of a degree), it is possible to detect even subtle angular change because the targets at Kwajalein are basically fixed and just a slight offset in antenna elevation will alter the rankings of the most intense reflectivities. In this particular case from 24

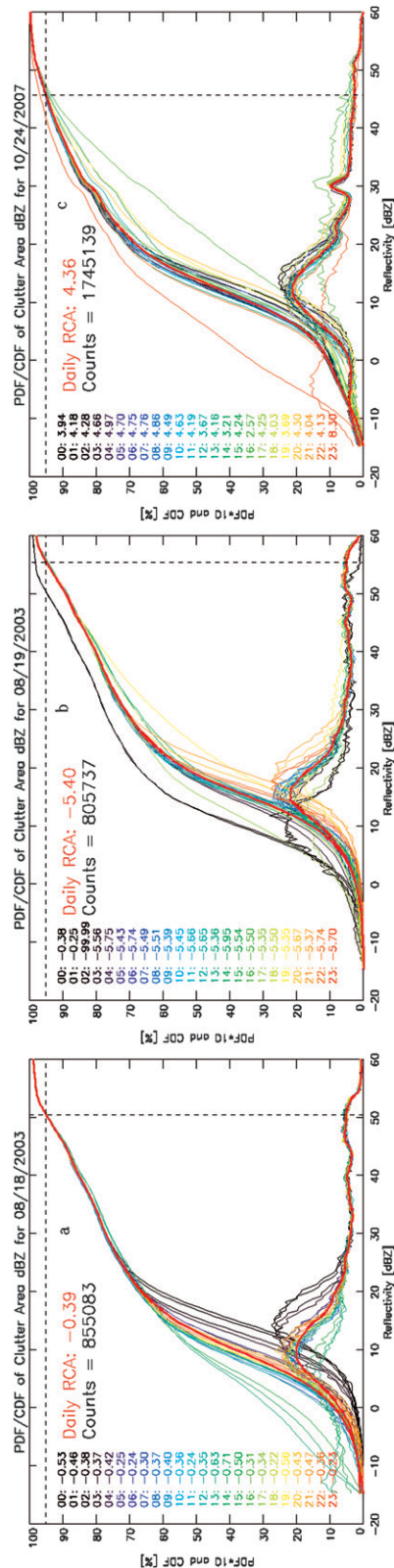


FIG. 5. Hourly and daily PDF/CDF plots of clutter area reflectivity showing distinction between a stable calibration day, a problem calibration day, and an antenna elevation irregularity day. Each curve is color coded by hour, and the ensemble or daily curve is shown by the bold red line. The RCA values, which represent the difference (in dB) between the current calibration and the baseline (set on 1 Aug 1999), are shown. The 95th percentile reflectivity is indicated by the intersection of the two dotted black lines, and “counts” represents the number of reflectivity points in the daily distribution. (a) Distributions from a stable calibration day with hour-to-hour fluctuation in RCA amounts less than 0.5 dB. Note the convergence in hourly PDFs and CDFs at the 95th percentile. (b) Distributions from a problem calibration day with RCA values significantly changing from the 0000 to the 0300 UTC hour. Note the *divergence* in hourly PDFs and CDFs at the 95th percentile. (c) Distributions from an antenna elevation irregularity day showing a significant fluctuation in hourly RCA values from the 2200 to 2300 UTC hours and divergence in hourly and daily distributions at the 95th percentile. Radar operators were notified of this RCA-detected irregularity and subsequently discovered a mechanical failure in the antenna hardware that caused an excessive beam overshoot.

TABLE 3. Ranking of gates in order of descending reflectivity magnitude to diagnose antenna elevation angle irregularity. The reflectivity distribution from the 15 most intense reflectivity gates from 2208 UTC (hourly RCA value of 4.1 dB) is substantially different from the top 15 gates from 2348 UTC (RCA value of 8.3 dB). Reflectivity gates are of lower intensity in the 2300 UTC hour, and the distances from the radar are much closer. The maximum range from the radar during the 2200 UTC hour is 15.8 km, and the lowest range is 1.2 km. However, during the 2300 UTC hour the maximum range is 1.6 km, whereas the lowest range is less than 1 km. The decreased reflectivity magnitude and closer distances in the 2300 UTC hour indicate that the antenna elevation angle has increased, and clutter targets at a farther range are being overshoot.

Rank	2208 UTC 24 Oct 2007			2348 UTC 24 Oct 2007		
	$Z_e$ (dBZ)	Azimuth ( $^\circ$ )	Distance (km)	$Z_e$ (dBZ)	Azimuth ( $^\circ$ )	Distance (km)
1	62.5	305	15.8	58.5	31	1.2
2	62.0	303	5.0	58.0	28	1.2
3	61.5	3	6.4	57.5	293	1.2
4	60.5	305	14.2	57.5	292	1.2
5	60.5	295	1.6	57.5	32	1.2
6	60.5	294	1.6	57.5	28	1.0
7	60.5	3	6.2	57.5	27	1.0
8	60.0	305	15.6	56.5	294	1.6
9	60.0	292	1.6	56.5	294	1.0
10	59.5	306	14.2	56.5	34	0.8
11	59.5	4	6.2	56.5	29	1.0
12	59.0	298	1.6	56.0	294	1.2
13	59.0	297	1.6	55.5	298	1.6
14	59.0	32	1.2	55.0	295	1.2
15	59.0	31	1.2	55.0	33	0.8

October 2007 (Fig. 5c), the RCA value increased by approximately +4 dB between the 2200 and 2300 UTC hours. Table 3 shows the ranking of individual gate returns from the 2200 and 2300 UTC hours. The wide discrepancy of reflectivity values with range indicates that the reflectivity distributions are drastically different between these two hours and that we are not sampling the same clutter area locations. There is an *approximate* empirical relationship of 1-dB RCA change to 0.1 $^\circ$  elevation angle change; therefore, in this case it was suspected that the antenna elevation increased by about 0.4 $^\circ$ . The radar engineer was not initially aware of an antenna elevation change. Subsequently, the engineer confirmed that a mechanical failure had occurred and the antenna angle had indeed changed. In this method, the RCA was used as a remote diagnostic tool to inform radar operators of a suspected problem.

### b. Practical application of the RCA

Figures 6a and 6b show timeline traces of the 95th percentile ensemble reflectivity distribution from the years 2000–01 and 2002–03, respectively. Periods of both radar stability and abrupt change are evident.

Some of the abrupt change episodes have been correlated with documented engineering events obtained from KPOL site logs provided by the former on-site contractor 3D Research Corporation. Note that because only some of the KPOL engineering logs were available for review and frequently the information lacked sufficient detail, several fluctuations in these timeline analyses are undocumented. These figures confirm that detected sensitivity changes are highly correlated with engineering events. Numerous gross corrections to KPOL reflectivity ( $\geq \pm 2$  dB) as identified by the RCA method from years 2000 through 2007 are shown in Table 4. Corrections are presented on a monthly scale to provide information on occurrence frequency; however, these changes usually do not occur gradually over the course of the month but typically occur on a more instantaneous scale. Months with two values represent those periods when two distinct fluctuations occurred. Corrections are determined by direct comparison of the 95th percentile reflectivity distributions with the established RCA baseline (Figs. 6a and 6b) and are computed as the amounts needed to adjust the 95th percentile to match the established baseline. The RCA method computes calibration adjustments on an hourly and daily basis using data from available volume scans during the period. Hourly RCA values are computed to monitor KPOL stability and to inform radar operators on a near-real-time basis as to when significant events occurred. Suspected radar stability issues are diagnosed and discussed in a timely manner with radar operators. Daily RCA values are used as corrections applied in the TSVO operational setting. The TRMM Ground Validation System (GVS) allows for application of calibration corrections through the “level 1” quality control (QC) algorithm (Kulie et al. 1999; Wolff et al. 2005). A QC parameter input file is generated with daily RCA corrections in addition to other adjustable QC parameters based on echo height and reflectivity thresholds. However, before the application of specific calibration corrections, the additional problem of antenna elevation angle change must be addressed. As shown in Fig. 5c and Table 3, unexpected changes in KPOL’s antenna elevation angle have a pronounced impact on the clutter area reflectivity distributions. Approximate antenna elevation angle changes and their effect on the RCA baseline are shown in Table 5. Those familiar with the history of KPOL operations will not be surprised by the magnitude of the angle changes. The significance of accounting for antenna elevation angle changes is quantified by an interim TSVO product (V6) for which RCA corrections were applied at face value *without* considering antenna irregularities. The consequence is that *all* RCA fluctuations were considered to be power related,

including those associated with antenna elevation angle changes. The resulting approximated power-law  $A$  coefficients and  $Z_e-R$  curves for V6 shown in Table 2 and Fig. 7 are more divergent than for V5 and clearly indicate that the interannual reflectivity distributions are not consistent. The antenna elevation angle had changed multiple times because of a suspected faulty electrical panel, use of a problematic release of a solar tracking utility, elevation drive motor failure, and operator troubleshooting adjustments. To properly account for antenna elevation angle change in RCA methodology, the calibration baseline is shifted by an amount equal to the magnitude of the change in the 95th percentile reflectivity from prior to and following antenna movement. A new calibration baseline is thus established, and this process repeats when the next antenna elevation angle change occurs. For example, if a known antenna angle increase (decrease) of  $0.5^\circ$  occurred and resulted in an approximate 5-dB decrease (increase) in the 95th percentile reflectivity distribution, then the RCA baseline would shift down (up) by a corresponding amount (5 dB). By shifting the RCA baseline in this manner, there is no change to the quantified calibration correction due to the antenna angle.

After adjusting the RCA baseline for antenna elevation angle changes, RCA calibration corrections are applied on a daily basis to adjust KPOL reflectivity to the revised baseline, and instantaneous quality-controlled radar and rain gauge data for entire years are then combined for WPMM distributions for V7 (current) product development. Table 2 and Fig. 8 show the V7 approximated  $Z_e-R$  power-law  $A$  coefficients and yearly WPMM  $Z_e-R$  curves from the years 2000 through 2007 respectively. There is significant improvement in the convergence of the  $Z_e-R$  curves and year-to-year agreement in the power-law coefficients. Slight variations in the curves may be related to factors such as the varying quantity of “good” rain gauges used by WPMM (see Amitai 2000 for combined gauge/radar QC and acceptance/rejection criteria) and the natural variability of rainfall within the scale of a radar pixel. Convergence of the  $Z_e-R$  curves is a clear indication that relative calibration stability from year to year has been significantly improved.

#### 4. Comparison with other correction methods

The research community has recognized the existence of calibration issues with KPOL and has developed other stabilization methods. The TRMM PR has been used as a stable standard for determining ground radar calibration biases (Schumacher and Houze 2000; AMD01; Houze et al. 2004). The echo area matching

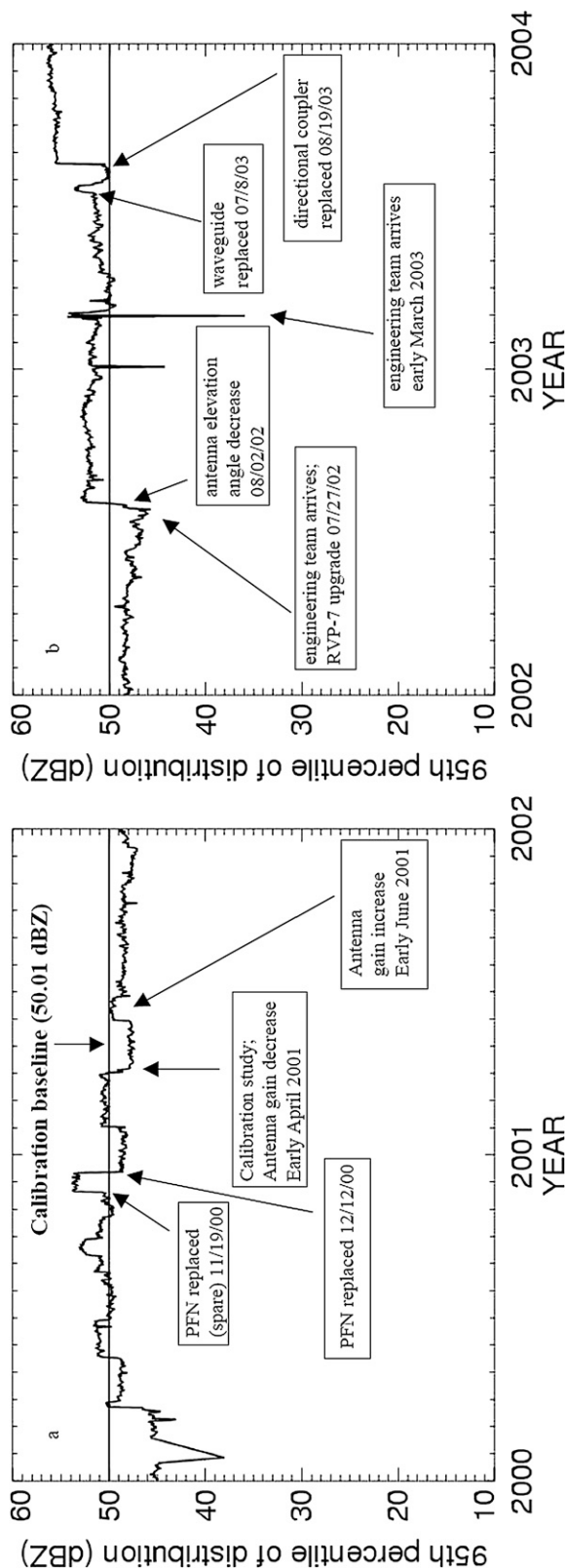


FIG. 6. Timeline of the correlation between the 95th percentile of ground clutter pixels and documented KPOL engineering events for years (a) 2000 and 2001 and (b) 2002 and 2003. The bold horizontal line near 50 dBZ represents the calibration baseline. PFN is the pulse forming network. Because of lack of information, some fluctuations are undocumented.

TABLE 4. Significant KPOL sensitivity fluctuations (approximate) for years 2000 through 2007 as detected by the RCA method. Calibration corrections (dB) are relative to the initial established baseline (50 dBZ). Dates with two values represent those months when two distinct fluctuations occurred. Radar events were corroborated with site engineering logs when available. The 2005 cascade failure data were not salvageable.

Date	Calibration correction (dB)	Reason
March 2000	+6	Annual calibration study—many changes
May 2000	+3	Unknown
June 2000	-2	Unknown
August 2000	+2	Pulse forming network replaced
September 2000	+3, -2	Unknown
November 2000	+4	PFN replacement
December 2000	-6	PFN replacement
February 2001	+3	Unknown
April 2001	-4	Annual calibration study
June 2001	+3, -2	Antenna gain changes/unknown
July 2002	+2	Waveguide replacement
July 2003	+2, -3	Waveguide replacement
August 2003	+6	Replaced directional coupler and loss change
April 2004	-9	Annual calibration study (power and elevation angle)
May 2004	+4	Change to directional coupler loss
July–December 2005	> 10	KPOL very unstable; cascade failure
January–December 2006	None	
February 2007	+2, -2	RCA sensitivity testing and validation
March 2007	+2	Computer systems upgrade

method developed by Schumacher and Houze (2000) and used in Houze et al. (2004) [hereafter collectively referred to as University of Washington (UW)] determines gross reflectivity calibration offsets by matching echo areas  $\geq 17$  dBZ from the PR and KPOL at the 6-km height level. This method relies on rainy temporal sampling of the PR and adjusts KPOL calibration offsets (with  $\pm 2$ -dB uncertainty) so that the KPOL echo area has the closest possible match with the echo area from the PR. Table 2 from Houze et al. (2004; not shown) presents calibration corrections from several years, and has good general agreement with RCA-determined corrections (Fig. 9). Based on PR overpass data, echo area matching, and a sphere calibration performed by NASA staff on board the NOAA Research Vessel (R/V) *Ron Brown*, it was determined that a calibration correction of +6 dB was required during the KWAJEX field campaign. The RCA method needed

TABLE 5. RCA baseline changes due to variation in antenna elevation angle. Baseline change was determined by change in the 95th percentile reflectivity distribution.

Date	Baseline (dB)	Comment
August 1999	50.01	Initial KWAJEX established baseline
August 2002	54.07	Antenna elevation decrease ( $\sim 0.41^\circ$ )
March 2003	52.82	Antenna elevation increase ( $\sim 0.12^\circ$ )
August 2004	54.24	Antenna elevation decrease ( $\sim 0.14^\circ$ )
January 2006	48.04	Antenna elevation increase ( $\sim 0.62^\circ$ )
June 2006	45.14	Antenna elevation increase ( $\sim 0.29^\circ$ )

an initial calibration baseline and therefore started with the same adjustment of +6 dB. Figure 9 shows agreement between the UW and RCA methods to within  $\pm 1$ –2 dB for most time periods, but because echo area matching relies on rainy PR overpasses, significant interoverpass calibration offsets are missed. January through August 2001 is a period in which the echo area matching method has missed calibration offsets because of the relatively poor temporal sampling of the PR.

AMD01 also determined ground radar calibration corrections based on comparisons with the TRMM PR. In their study, PR and KPOL (referred to as KWAJEX-S) reflectivities were interpolated and statistically matched in a common three-dimensional Cartesian grid. Their data analysis (August–December 1999) of stratiform echo showed that a calibration correction of approximately +6 to +7 dB needed to be applied to KWAJEX-S. Agreement of calibration corrections from both the area echo matching method (UW) and mean reflectivity differences (AMD01) provides an initial degree of assurance that KPOL was indeed running “cold” at the beginning of the KWAJEX experiment (August 1999). As in the UW method of area echo matching, the calibration corrections from AMD01 based on mean reflectivity differences rely on coincident TRMM sampling during rain, so significant calibration corrections can be missed. In addition, neither UW echo area matching nor AMD01 mean reflectivity difference methods can detect changes in antenna elevation angle. In contrast, after establishing the initial RCA calibration baseline on 1 August 1999 (50.01 dBZ), the status of KPOL calibration is being closely monitored and calibration offsets are being measured on a continuous hour-by-hour near-real-time basis by the RCA method *without* dependence on PR observations. Section 3 detailed convergence of the TSVO V7 WPMM  $Z_e$ - $R$  reflectivity distributions through coefficients (Table 2) and graphically through the resulting curves (Fig. 8). The next section quantifies the improved stability of V7 RCA corrected reflectivity over V5 through comparison of mean reflectivity differences with the TRMM PR.

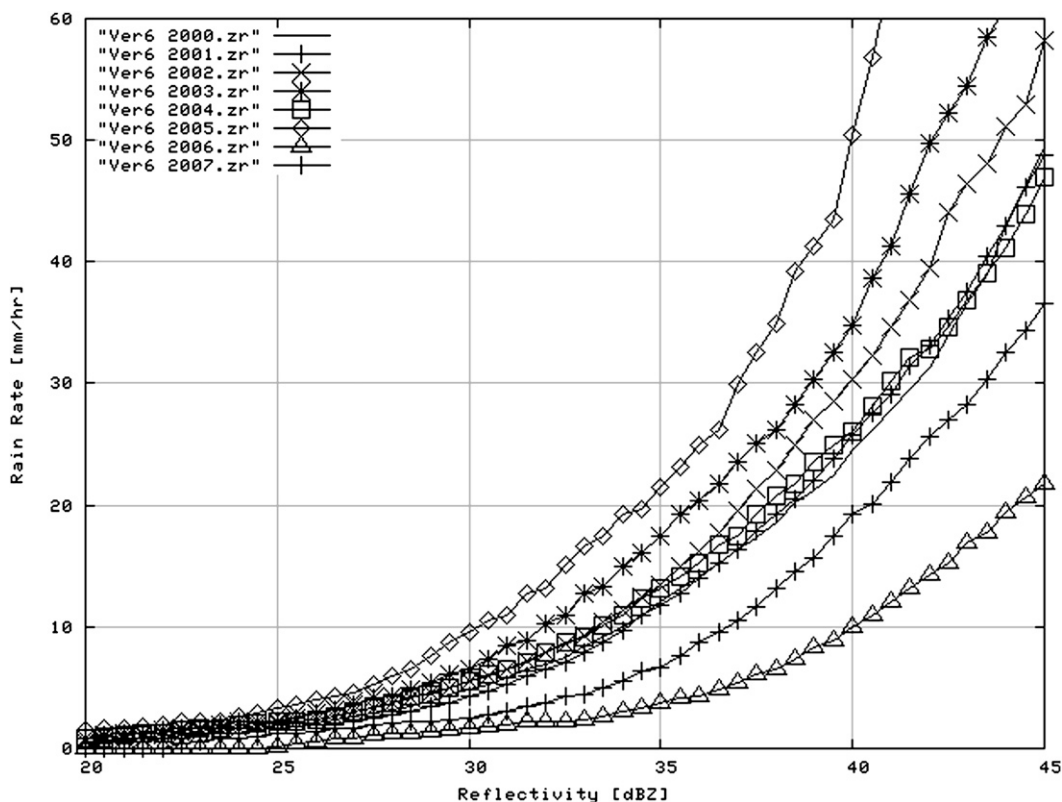


FIG. 7. TSOV GV V6 WPMM yearly  $Z_e$ - $R$  curves from 2000 to 2007. The V6 curves have RCA corrections applied. All corrections were considered to be related to power calibration. The divergence in curves shows the effect of antenna elevation change on the clutter area reflectivity distributions.

### 5. Improved stability of RCA-corrected KPOL reflectivity

It is emphasized that it is not the intention of this paper to validate PR reflectivity measurements but instead to show improved stability in corrected KPOL reflectivity using the PR as a stable reference; therefore, the *fluctuation* of the mean differences between instruments is much more important to this study than the absolute magnitude of the differences themselves. Readers interested in studies validating TRMM estimates are referred to Datta et al. (1999), Schumacher and Houze (2000), Nicholson et al. (2003), Fisher (2004), and Wolff and Fisher (2008). The multiple panels of Fig. 10 show monthly and yearly mean difference (offset) between PR attenuation-corrected 2A25 V6 stratiform reflectivity and RCA-corrected KPOL 2A55 V7 stratiform reflectivity for rainy overpasses from 2000 through 2007. This is the same type of analysis presented for the V5 comparison in section 2b. Month-to-month fluctuations in mean differences over the eight years are on the order of  $\pm 1$ – $2$  dB (with some exceptions). Yearly mean differences fluctuate by approximately  $\pm 1$  dB (with

95% CI bounds within established PR uncertainty), and standard deviations about the mean differences from all yearly observations range from 3.4 to 3.8 dB (an improvement over the V5 standard deviation range of 3.5–4.3 dB). If measurement uncertainty in RCA corrections is  $\pm 0.5$  dB, uncertainty in corrected KPOL radar reflectivity is  $\pm 1.0$  dB, and uncertainty in the PR reflectivity is  $\pm 1$  dB, then we would expect standard deviations about the mean differences to be within approximately  $\pm 2.5$  dB. The amount of variability beyond this range is believed to be from factors discussed in Bolen and Chandrasekar (2003), specifically, time synchronization mismatches between datasets (8-min window), geometrical distortions from platform and TRMM attitude perturbations, and possible residual errors in resolution volume matching. However, these sources of error exist in both V5 and V7 comparisons, and therefore do not significantly affect the intended focus of showing improved KPOL stability. By comparing the V5 results (Fig. 4) with the V7 results (Fig. 10), significant improvement in stability is shown, especially in years with known calibration issues (2000, 2001, and 2003). Sample size issues are again a limiting factor in

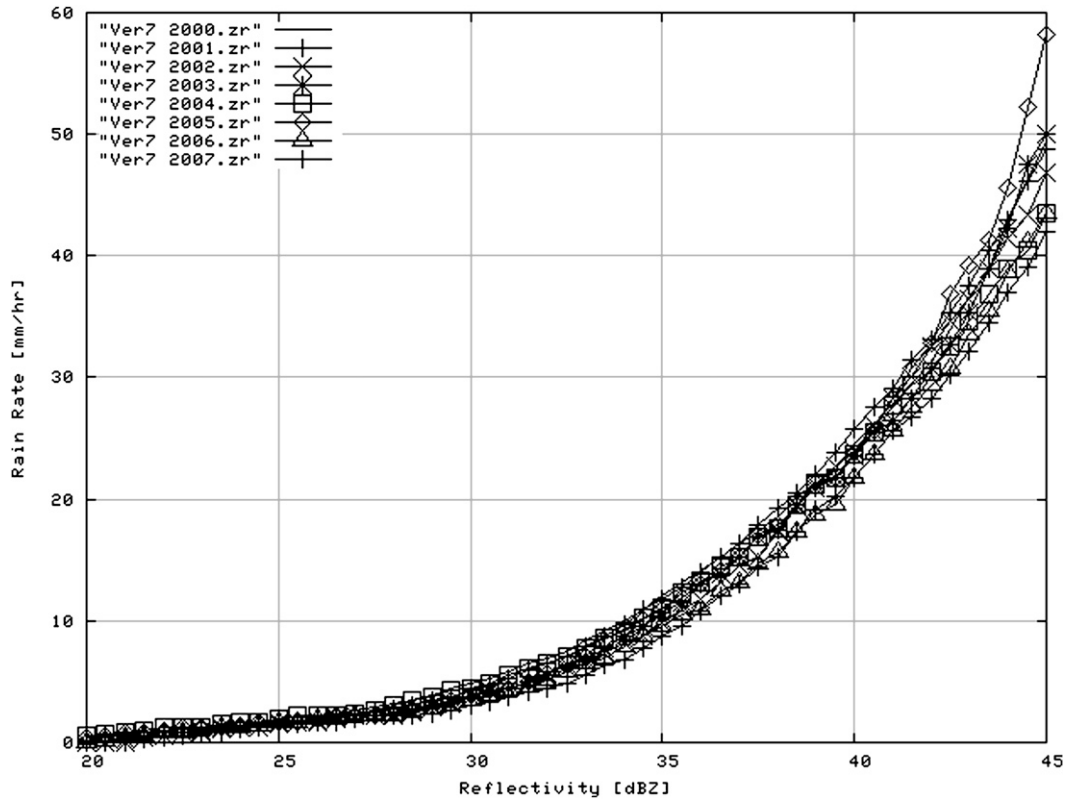


FIG. 8. TSVO GV V7 WPMM yearly  $Z_e$ - $R$  curves from 2000 to 2007. The V7 curves have both RCA and antenna elevation angle corrections applied. Convergence in the  $Z_e$ - $R$  curves is the expected result and signifies that WPMM is using stable reflectivity distributions. Minor year-to-year curve variation may be due to the natural variability of rainfall.

the dry season (January–March) of each year; therefore, comparisons from these months have reduced confidence and are not considered reliable. Reviewing year 2003 in closer detail shows an intermonth variability spread in mean differences of 5 dB in V5 (+2 dB in May to -3 dB in December), whereas in V7, the intermonth variability spread is approximately 1.5 dB (+0.5 dB in May to -1 dB in December). Figure 11 shows V5 and V7 scatterplots of radar and rain gauge WPMM-estimated rainfall from year 2003. In August 2003, the replacement of a directional coupler with an associated loss change resulted in a +6-dB increase to the 95th percentile reflectivity distribution (as shown in Fig. 6b and Table 4). The V5 scatterplot (Fig. 11a) depicts the broad uncorrected distribution used to develop the 2003  $Z_e$ - $R$  lookup table. A key statistic for comparison is the normalized mean absolute deviation (MAD) between radar and rain gauge estimated accumulations, defined as

$$MAD = \frac{\mu_{|G-R|}}{\mu_G}, \quad (4)$$

where  $\mu$  is the statistical average,  $G$  is the gauge accumulation, and  $R$  is the radar-estimated accumulation.

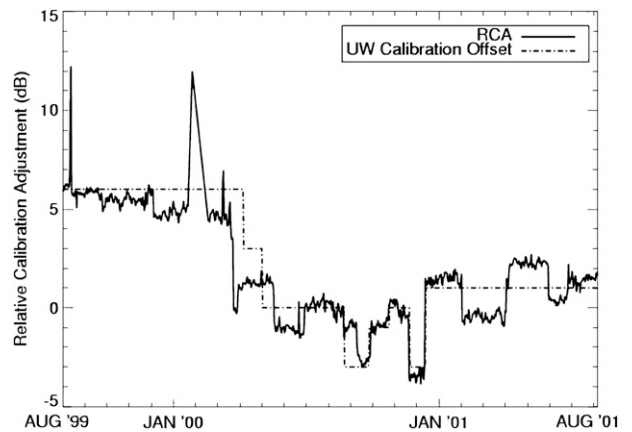


FIG. 9. Comparison between RCA and UW calibration offsets (from SW08). The RCA method is based on using KPOL ground clutter returns to determine calibration offsets, whereas the UW method uses echo area matching between the TRMM PR and KPOL. Agreement is generally within  $\pm 1$ -2 dB; however, calibration fluctuations are missed by the echo area matching method due to the temporal sampling of the PR.

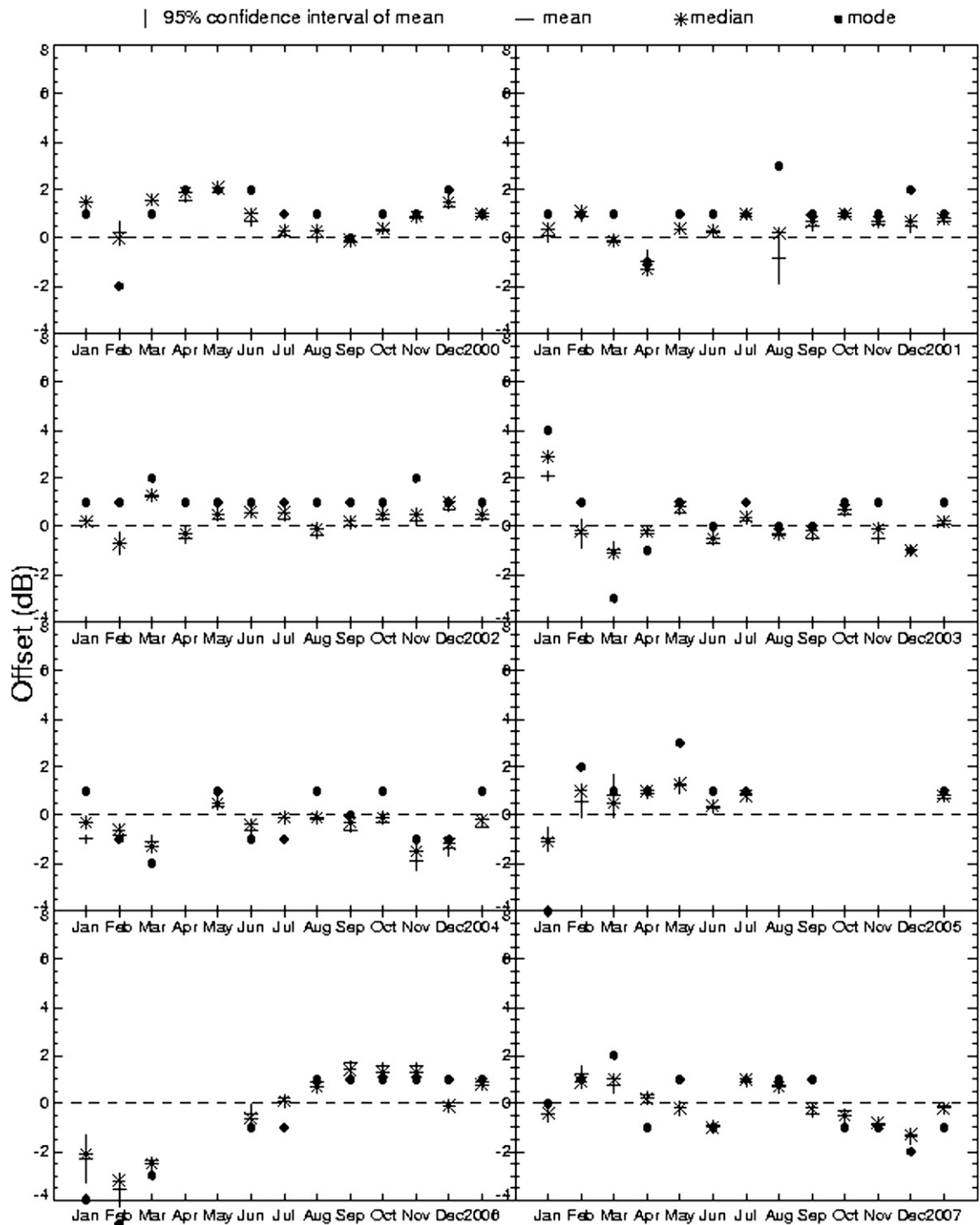


FIG. 10. Monthly and yearly comparison of mean reflectivity difference (offset) between the TRMM PR (2A25, V6) and TSVO KPOL (2A55, V7) from years 2000 through 2007. The final column in each panel is for the entire year. Increased offsets in January through March of each year are related to limited sample size in the dry season.

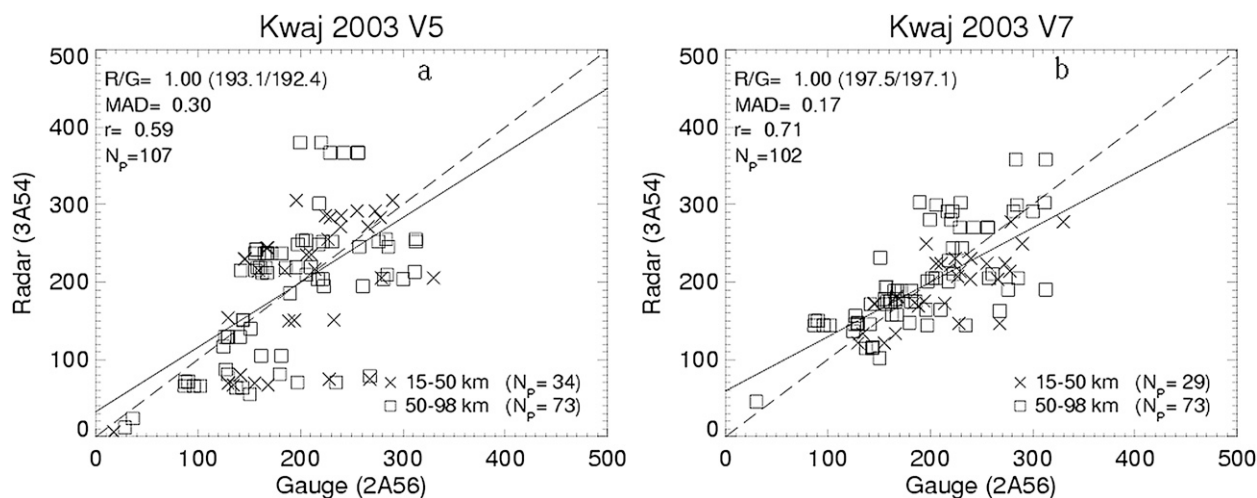


FIG. 11. The V5 and V7 yearly scatterplots of radar and rain gauge WPMM-estimated rainfall from the year 2003. To increase sample size and provide robust statistics, data are compiled on a monthly basis and combined for yearly plots. TSP 3A54 is the monthly rainfall estimate from the radar using the WPMM-derived  $Z_e$ - $R$  lookup table from 2003. The monthly rain gauge data (TSP 2A56) are dependent; therefore, the radar-to-gauge (R/G) accumulation ratio is near unity. Here  $N_p$  represents the total number of monthly points (rain gauges) used in the analysis. The dashed line in each panel is a one-to-one correspondence line; the solid lines represent a least squares fit regression. (a) A significant calibration event occurred on 19 Aug 2003 with the replacement of a directional coupler (see Fig. 6b) and resulted in a broad reflectivity distribution for WPMM matching. This is reflected in the mean absolute deviation and correlation ( $r$ ) statistics. (b) After RCA correction, the consistency of the reflectivity distribution for WPMM matching has significantly improved as shown by the statistics and reduced scatter.

The MAD improves from 0.30 in V5 to 0.17 with the RCA-corrected V7 distribution (Fig. 11b); the correlation ( $r$ ) jumps from 0.59 to 0.71 with the corrected data. In years with significant calibration corrections, the statistical improvement in WPMM distributions is dramatic, as shown in the 2003 example. In years with more subtle calibration changes, the improvement is slight but still present. Application of the RCA method has imparted significant stability to the reflectivity distributions, which is a requirement for consistent WPMM rain-rate estimation. The fluctuations in corrected KPOL reflectivity distributions (V7) as compared to the TRMM PR are significantly less than prior version statistics; they are comparable to the established calibration and uncertainty boundaries of the TRMM PR. With the assistance of available radar engineering logs, the RCA technique has been retroactively applied to KPOL data from January 2000 through December 2007, effectively salvaging eight years of reflectivity data for the research community.

## 6. Summary

The KPOL radar on Kwajalein Island has been designated as a primary ground validation instrument for TRMM. Unfortunately, KPOL has had a long history of calibration and antenna angle uncertainty since the TRMM satellite launch in November 1997. A brief his-

tory of KPOL data and historical correction attempts from the GSFC GV program has been presented. The TSVO developed a unique approach, the relative calibration adjustment (RCA) method, to monitor radar sensitivity fluctuations using statistical ensemble characteristics of ground clutter returns. The V7 GV reflectivity products (1C51 and 2A55) have been corrected for both calibration and elevation angle errors using the RCA method, which has significantly improved the stability in reflectivity distributions (over V5 products) required for WPMM reflectivity-rain-rate table development and for climatological and physical characterization studies. The improved stability is quantified by comparison of mean reflectivity differences with a recognized stable standard, the TRMM PR. The variation of interyear mean reflectivity differences between the attenuation-corrected TRMM PR 2A25 V6 reflectivity and TSVO KPOL 2A55 V7 reflectivity are on the order of  $\pm 1$  dB. This is within expected error bounds and comparable to the estimated uncertainty of the PR, while the 95% CI bounds of these measurements are within the estimated uncertainty of the PR. Radar-rain gauge accumulation scatterplots have confirmed the improved stability in reflectivity distributions. Therefore, we confidently state that the RCA method has provided the calibration stability needed for significantly improved WPMM rain-rate estimation from Kwajalein. The RCA method has salvaged over eight years of

KPOL data that would otherwise have been unusable and has provided a remote diagnostic tool to assist data analysts and radar operators in detecting sensitivity and angle changes both historically and in currently observed data. The RCA method may be extensible to other research radars that do not use ground clutter or velocity notch filters prior to data recording. Future research includes investigation of KPOL's dual-polarimetric capability to provide absolute calibration, hydrometeor identification, and rain-rate estimation. The RCA method will be used to independently validate calibration adjustments obtained through dual-polarimetric measurements. V7 reflectivity and rain-rate products are available from the Goddard Earth Sciences Data and Information Services Center (GES DISC; <http://disc.gsfc.nasa.gov>). Further information and near-real-time RCA distributions are available from the TRMM validation site ([http://trmm-fc.gsfc.nasa.gov/trmm\\_gv](http://trmm-fc.gsfc.nasa.gov/trmm_gv)).

*Acknowledgments.* The authors thank Dr. Ramesh Kakar (NASA Headquarters), Mr. Richard Lawrence (Chief, NASA/GSFC TRMM Satellite Validation Office), Dr. Scott Braun (TRMM Project Scientist), and Dr. Robert Adler (former TRMM Project Scientist) for their support of this effort. We thank Dr. David Atlas for his contributions and helpful discussions on RCA theory. We also acknowledge assistance from TRMM Satellite Validation Office support staff, including David Makofski, Bart Kelley, and Marcella (Lynne) Shupp. This research was supported by NASA Grant NNG07EJ50C.

#### REFERENCES

- Amitai, E., 2000: Systematic variation of observed radar reflectivity–rainfall rate relations in the tropics. *J. Appl. Meteor.*, **39**, 2198–2208.
- , D. A. Marks, D. B. Wolff, D. S. Silberstein, B. L. Fisher, and J. L. Pippitt, 2006: Evaluation of radar rainfall products: Lessons learned from the NASA TRMM validation program in Florida. *J. Atmos. Oceanic Technol.*, **23**, 1492–1505.
- Anagnostou, E. N., C. A. Morales, and T. Dinku, 2001: The use of TRMM precipitation radar observations in determining ground radar calibration biases. *J. Atmos. Oceanic Technol.*, **18**, 616–628.
- Awaka, J., T. Iguchi, H. Kumagai, and K. Okamoto, 1997: Rain type classification algorithm for TRMM precipitation radar. *Proc. Int. Geoscience and Remote Sensing Symp.*, Suntec City, Singapore, IEEE, 1633–1635.
- Blossey, P. N., C. S. Bretherton, J. Cetrone, and M. Kharoutdinov, 2007: Cloud-resolving model simulations of KWJEX: Model sensitivities and comparisons with satellite and radar observations. *J. Atmos. Sci.*, **64**, 1488–1508.
- Bolen, S. M., and V. Chandrasekar, 2000: Quantitative cross validation of space-based and ground-based radar observations. *J. Appl. Meteor.*, **39**, 2071–2079.
- , and —, 2003: Methodology for aligning and comparing spaceborne radar and ground-based radar observations. *J. Atmos. Oceanic Technol.*, **20**, 647–659.
- Cetrone, J., and R. A. Houze Jr., 2006: Characteristics of tropical convection over the ocean near Kwajalein. *Mon. Wea. Rev.*, **134**, 834–853.
- Datta, S., B. Roy, L. Jones, T. Kasparis, P. Ray, and D. Charalampidis, 1999: Evaluation of TRMM precipitation radar rainfall estimates using NEXRAD and rain gauges in central and south Florida. Preprints, *29th Int. Conf. on Radar Meteorology*, Montreal, QC, Canada, Amer. Meteor. Soc., 754–757.
- Fisher, B. L., 2004: Climatological validation of TRMM TMI and PR monthly rain products over Oklahoma. *J. Appl. Meteor.*, **43**, 519–535.
- Holder, C., S. E. Yuter, A. Sobel, and A. Ayyer, 2008: The mesoscale characteristics of tropical oceanic precipitation during Kelvin and mixed Rossby–gravity wave events. *Mon. Wea. Rev.*, **136**, 3446–3464.
- Houze, R. A., Jr., S. Brodzik, C. Schumacher, S. Yuter, and C. R. Williams, 2004: Uncertainties in oceanic radar rain maps at Kwajalein and implications for satellite validation. *J. Appl. Meteor.*, **43**, 1114–1132.
- Iguchi, T., T. Kozu, R. Meneghini, J. Awaka, and K. Okamoto, 2000: Rain-profiling algorithm for the TRMM precipitation radar. *J. Appl. Meteor.*, **39**, 2038–2052.
- Joss, J., and A. Waldvogel, 1967: Ein spectrograph für Niederschlagsstropfen mit automatischer Auswertung (A spectrograph for the automatic analysis of raindrops). *Pure Appl. Geophys.*, **69**, 240–246.
- Kozu, T., and Coauthors, 2001: Development of precipitation radar onboard the Tropical Rainfall Measuring Mission (TRMM) satellite. *IEEE Trans. Geosci. Remote Sens.*, **39**, 102–116.
- Kulie, M. S., M. Robinson, D. A. Marks, B. S. Ferrier, D. Rosenfeld, and D. B. Wolff, 1999: Operational processing of ground validation data for the Tropical Rainfall Measuring Mission. Preprints, *29th Int. Conf. on Radar Meteorology*, Montreal, QC, Canada, Amer. Meteor. Soc., 736–739.
- Kummerow, C., W. Barnes, T. Kozu, J. Shiue, and J. Simpson, 1998: The Tropical Rainfall Measuring Mission (TRMM) sensor package. *J. Atmos. Oceanic Technol.*, **15**, 809–817.
- Marks, D. A., and Coauthors, 2000: Climatological processing and product development for the TRMM ground validation program. *Phys. Chem. Earth*, **25B**, 871–876.
- Mohr, C. G., and R. L. Vaughan, 1979: An economical procedure for Cartesian interpolation and display of reflectivity factor data in three-dimensional space. *J. Appl. Meteor.*, **18**, 661–670.
- Nicholson, S. E., and Coauthors, 2003: Validation of TRMM and other rainfall estimates with a high-density gauge dataset for West Africa. Part II: Validation of TRMM rainfall products. *J. Appl. Meteor.*, **42**, 1355–1368.
- Probert-Jones, J. R., 1962: The radar equation in meteorology. *Quart. J. Roy. Meteor. Soc.*, **88**, 485–495.
- Rinehart, R. E., 1978: On the use of ground return targets for radar reflectivity factor calibration checks. *J. Appl. Meteor.*, **17**, 1342–1350.
- Rosenfeld, D., D. Atlas, D. B. Wolff, and E. Amitai, 1992: Beamwidth effects on Z-R relations and area-integrated rainfall. *J. Appl. Meteor.*, **31**, 454–464.
- , D. B. Wolff, and E. Amitai, 1994: The window probability matching method for rainfall measurements with radar. *J. Appl. Meteor.*, **33**, 682–693.
- Schumacher, C., and R. A. Houze Jr., 2000: Comparison of radar data from the TRMM satellite and Kwajalein oceanic validation site. *J. Appl. Meteor.*, **39**, 2151–2164.

- Silberstein, D. S., D. B. Wolff, D. A. Marks, D. Atlas, and J. L. Pippitt, 2008: Ground clutter as a monitor of radar stability at Kwajalein, RMI. *J. Atmos. Oceanic Technol.*, **25**, 2037–2045.
- Sobel, A. H., S. E. Yuter, C. S. Bretherton, and G. N. Kiladis, 2004: Large-scale meteorology and deep convection during TRMM KWAJEX. *Mon. Wea. Rev.*, **132**, 422–444.
- Steiner, M., R. A. Houze Jr., and S. E. Yuter, 1995: Climatological characterization of three-dimensional storm structure from operational radar and rain gauge data. *J. Appl. Meteor.*, **34**, 1978–2007.
- Tokay, A., P. G. Bashor, E. Habib, and T. Kasparis, 2008: Raindrop size distribution measurements in tropical cyclones. *Mon. Wea. Rev.*, **136**, 1669–1685.
- Ulbrich, C. W., and L. G. Lee, 1999: Rainfall measurement error by WSR-88D radars due to variations in  $Z$ - $R$  law parameters and the radar constant. *J. Atmos. Oceanic Technol.*, **16**, 1017–1024.
- Wang, J., B. L. Fisher, and D. B. Wolff, 2008: Estimating rain rates from tipping-bucket rain gauge measurements. *J. Atmos. Oceanic Technol.*, **25**, 43–56.
- Wilks, D. S., 1995: *Statistical Methods in the Atmospheric Sciences*. 1st ed. Academic Press, 467 pp.
- Wolff, D. B., and Coauthors, 2005: Ground validation for the Tropical Rainfall Measuring Mission (TRMM). *J. Atmos. Oceanic Technol.*, **22**, 365–380.
- , and B. L. Fisher, 2008: Comparisons of instantaneous TRMM ground validation and satellite rain-rate estimates at different spatial scales. *J. Appl. Meteor. Climatol.*, **47**, 2215–2237.
- Yuter, S. E., R. A. Houze Jr., E. A. Smith, T. Wilheit, and E. Zipser, 2005: Physical characterization of tropical oceanic convection observed in KWAJEX. *J. Appl. Meteor.*, **44**, 385–415.